*Int. J. Electrochem. Sci.*, 8 **(2013)** 2826 - 2841

International Journal of
ELECTROCHEMICAL
SCIENCE
www.electrochemsci.org

# Synthesis, Characterization, and Vitamin C Detection of a Novel L-Alanine-Modified PEDOT with Enhanced Chirality

*Baoyang Lu,*[1,2] *Yao Lu,*[1] *Yangping Wen,*[3] *Xuemin Duan,*[*1] *Jingkun Xu,*[*1,2] *Shuai Chen,*[1] *and Long Zhang*[1]

[1] School of Pharmacy, Jiangxi Science & Technology Normal University, Nanchang, 330013, P R China
[2] School of Materials Science & Engineering, Shandong University, Jinan, 250061, P R China
[3] Key Laboratory of Crop Physiology, Ecology & Genetic Breeding, Ministry of Education and Jiangxi Province, Jiangxi Agricultural University, Nanchang, 330045, P R China
[*]E-mail: duanxuemin@126.com; xujingkun@tsinghua.org.cn

*Received:* 16 December 2012 / *Accepted:* 6 January 2013 / *Published:* 1 February 2013

A novel chiral L-alanine-modified 3,4-ethylenedioxythiophene (EDOT) precursor, (2S)-(2,3-dihydrothieno[3,4-*b*][1,4]dioxin-2-yl)methyl 2-(*tert*-butoxy carbonylamino)propanoate (EDOT-Boc-Ala), was synthesized and electropolymerized in $CH_2Cl_2$–$Bu_4NBF_4$. The corresponding polymer, poly((2S)-(2,3-dihydrothieno[3,4-*b*][1,4]dioxin-2-yl)methyl 2-(*tert*-butoxy carbonylamino)propanoate) (PEDOT-Boc-Ala) film showed good redox activity and stability. The electrochemical behavior, structural characterization, chirality, solubility, spectroscopic properties, thermal stability, and morphology of PEDOT-Boc-Ala film were investigated. Both doped and dedoped PEDOT-Boc-Ala film could well dissolve in strong polar solvents such as dimethyl sulfoxide, tetrahydrofuran, and acetone, etc. The determination of specific rotation showed that the electropolymerization of EDOT-Boc-Ala did not influence its conformation and the polymer exhibited an enhanced specific rotation ($[\alpha]^{20.0}$ = -191.08$^o$) in comparison with that of the monomer ($[\alpha]^{20.0}$ = -30.77$^o$). Moreover, the amperometric biosensor based on PEDOT-Boc-Ala film (as immobilization matrix of biologically-active species) was successfully fabricated and employed to determine the concentration of vitamin C.

**Keywords:** Chiral conducting polymers; Amino acids modified PEDOT; Electropolymerization; Amperometric biosensor; Vitamin C determination

## 1. INTRODUCTION

The development and application of chiral conducting polymers with well-defined structure have attracted considerable interest because of their potential use in chiral separation, chiral sensors, optoelectronic devices, batteries, and asymmetric catalysis [1-10]. Interestingly, the optically inactive

chiral conducting polymers could become chiral by the addition of a chiral guest, showing that the introduction of chirality could also be a result of the main-chain chirality, such as a predominantly one-handed helical structure with a preferred twist reflecting the stereochemistry of the chiral guest induced by a acid-base complexation between the conjugated polymer and the chiral guest [11-13]. There are several methods to induce chirality into conducting polymers. One of them is the usage of both liquid crystalline conducting polymers and chiral dopants [14-16]. Another is the polymerization of a chiral monomer in an asymmetric reaction field consisting of chiral nematic liquid crystal [17-22]. Besides, the introduction of chiral moiety into the side chain of conducting polymers is also an important way to introduce chirality [23-36].

It is well-known that poly(3,4-ethylenedioxythiophene) (PEDOT) is one of the most stable conducting polymers with versatile functional properties such as high electrical conductivity, low band gap, good redox activity, high thermal stability, and excellent transparency in the doped state [37-38]. Unfortunately, PEDOT shows no fluorescence emission peaks in the whole visible region [39] and chiral property, which limited its wide application as fluorescent and chiral materials. Therefore, the design and synthesis of novel PEDOT derivatives with unique properties in order to overcome these defects and obstacles are still very necessary and significant and apparently also a considerable challenge.

On the other hand, the natural chiral molecules, amino acids, are crucial to life and have scores of functions. One particularly chief function of amino acids is to serve as the building blocks of protein in the body. In addition, all natural amino acids (with the exception of glycine) have the three-dimensional ordered structure, and excellent biocompatibility, low toxicity, efficient and quick biodegradability. Hence, the natural amino acids and their derivatives are ideal precursor materials for the design and synthesis of chiral polymers by introducing the chiral moieties into the side chain of the polymer. However, to the best of our knowledge, there have so far been no reports on the grafting of the natural amino acids onto PEDOT derivatives.

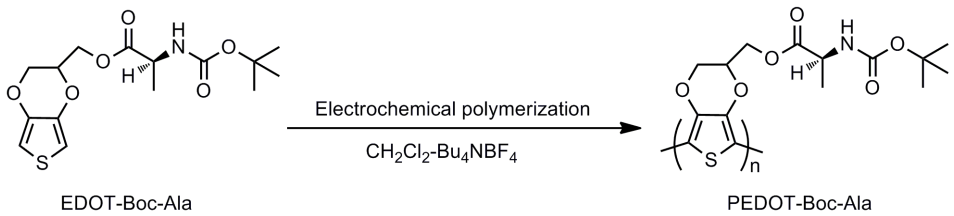


**Scheme 1.** The chemical structure of EDOT-Boc-Ala monomer and its polymer, together with its electrochemical polymerization.

In this work, N-Boc-L-amino acid was introduced as the side chain moiety into PEDOT through covalent bonding. A novel PEDOT derivative, poly((2S)-(2,3-dihydrothieno[3,4-b][1,4]dioxin-2-yl)methyl 2-(*tert*-butoxy carbonylamino)propanoate) (PEDOT-Boc-Ala, Scheme 1), was designed and synthesized for the first time through the electropolymerization of the synthesized precursor (2S)-(2,3-dihydrothieno[3,4-b][1,4]dioxin-2-yl)methyl 2-(*tert*-butoxy carbonylamino)propanoate (EDOT-Boc-Ala) (Scheme 2). Further, the electrochemical behavior,

structural characterization, chirality, solubility, spectroscopic properties, thermal stability, and morphology of the as-prepared PEDOT-Boc-Ala film were investigated in detail. Also, the amperometric biosensor based on PEDOT-Boc-Ala film was successfully fabricated and employed for the determination of vitamin C.

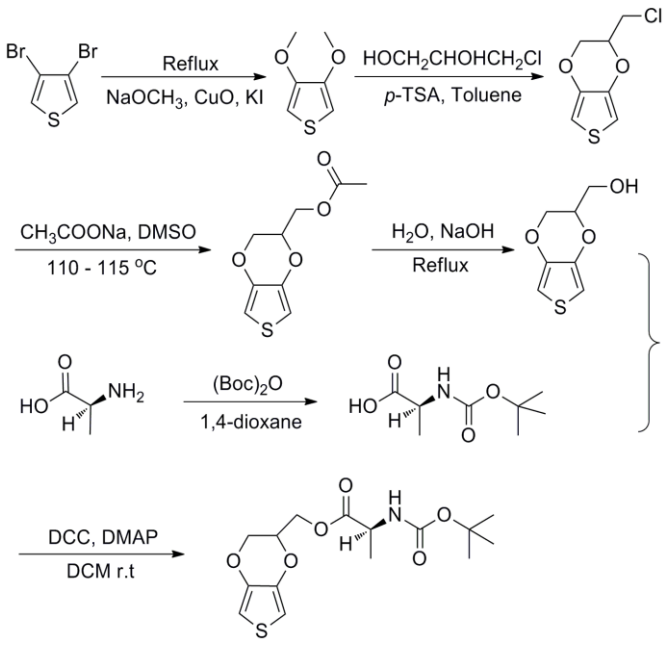


**Scheme 2.** The synthesis route of EDOT-Boc-Ala

## 2. EXPERIMENTAL

### *2.1. Materials*

3,4-Dibromothiophene (98%; Shanghai Bangcheng Chemical Co., Ltd), copper(ii) oxide (CuO, 98%; Tianjin Damao Chemical Reagent Factory), potassium iodide (KI, 98%; Shanghai Chemical Reagent Co., Ltd.), sodium methoxide, 3-chloro-1,2-propanediol (Wuhan Remote Technology Development Co., Ltd.), sodium acetate, *p*-toluenesulfonic acid (≥99.5%; Tianjin Damao Chemical Reagent Factory), L-alanine (99%; Aladdin Chemistry Co. Ltd), N,N'-dicyclohexyl carbodiimide (DCC, 99%; Aladdin Chemistry Co. Ltd), 4-dimethylaminopyridine (DMAP, 99%; Aladdin Chemistry Co. Ltd), di-*tert*-butyl dicarbonate ($(Boc)_2O$, 99%; Aladdin Chemistry Co. Ltd), and dimethyl sulfoxide (DMSO, analytical grade; Tianjin Bodi Chemicals Co., Ltd) were used as received. Dichloromethane (DCM, analytical grade; Tianjin Damao Chemical Reagent Factory) was purified by distillation over calcium hydride before use. Tetrabutylammonium tetrafluoroborate ($Bu_4NBF_4$, 99%; Acros Organics) was dried under vacuum at 60 °C for 24 h before use. Ascorbate oxidase (AO, from Cucurbita sp, 250 U $g^{-1}$) was purchased from Sigma. 5% Nafion solution was obtained from DuPont Co., Ltd. Disodium hydrogen phosphate dodecahydrate ($Na_2HPO_4 \cdot 12H_2O$), and sodium dihydrogen phosphate dihydrate ($NaH_2PO_4 \cdot 2H_2O$) were purchased from Sinopharm Chemical Reagent Co., Ltd.

50 mM Phosphate-buffered solution (PBS, pH 6.5) was prepared from 50 mM $NaH_2PO_4 \cdot 2H_2O$ and 50 mM $Na_2HPO_4 \cdot 12H_2O$. L-ascorbic acid (vitamin C, AA) was purchased from Bio Basic Inc. Other reagents were all A.R. grade and used as received without further treatment.

### *2.2 Syntheses*

#### *2.2.1 3,4-dimethoxythiophene* [40]

To a three-necked flask equipped with an nitrogen purge, sodium methoxide (20.80 g, 28% mass fraction, 107.81 mmol), 3,4-dibromothiophene (5.00 g, 20.67 mmol), copper(ii) oxide (16.50 g, 207.42 mmol), potassium iodide (1.37 g, 8.25 mmol), and methanol (20 mL) were added. The mixture was refluxed for three days. Then, another sodium methoxide (20.80 g, 107.81 mmol) was added, and the solution was refluxed for another one day and was then cooled to room temperature and filtered. The filter cake was rinsed with ether and the filtrate was poured into 50 mL water. The solution was then extracted with ether. The organic fractions were combined and dried with magnesium sulfate. After removal of the solvent, the remaining crude product was isolated by flash chromatography (silica gel, petroleum ether) to give 2.62 g of a colorless oil (yield 88.0%). $^1$H NMR (400 MHz, $CDCl_3$): δ 6.19 (s, 2H), 3.86 (s, 6H).

#### *2.2.2 EDOT-MeCl* [41-42]

To a three-necked flask equipped with an nitrogen purge, 3,4-dimethoxythiophene (1.44 g, 9.99 mmol), 3-chloro-1,2-propanediol (2.45 g, 22.16 mmol), *p*-toluene sulfonic acid (0.15 g, 0.87 mmol), and dry toluene (27 mL) were added. The solution was heated at 90 °C for 24 h. Then, another of diol (2.45 g, 22.16 mmol) was added, and the solution was heated at 90 °C for another 3 h and was allowed to cool to room temperature. After removal of the solvent, the remaining crude product was isolated by flash chromatography (silica gel, hexane/dichloromethane, 8/2, v/v) to give 1.18 g of a white solid (yield 62.0%). $^1$H NMR (400 MHz, $CDCl_3$): δ 6.37 (s, 2H), 4.35-4.40 (m, 1H), 4.27-4.35 (m, 1H), 4.14-4.18 (m, 1H), 3.65-3.75 (m, 2H).

#### *2.2.3 EDOT-MeOH* [40]

To a three-necked flask, EDOT-MeCl (1.91 g, 10.02 mmol), sodium acetate (1.25 g, 15.24 mmol), and DMSO (30 mL) were added. The solution was stirred for 1 h at 120 °C. The mixture was poured into water and extracted with DCM. After removing DCM under reduced pressure, a light yellow oil, (2,3-dihydrothieno[3,4-*b*][1,4]dioxin-2-yl)methyl acetate (EDOT-MeOAc), was obtained, and used in the next step without purification.

To a round bottom f1ask equipped with a reflux condenser, EDOT-MeOAc was added to a solution of NaOH (1.40 g, 35.0 mmol) in water (40 mL). The mixture was refluxed for 1 h and then cooled to room temperature. Then, 22 mL of water was added. The mixture was acidified, and then

extracted with DCM. The solvent was removed under reduced pressure and column chromatography (hexane/dichloromethane, 8/2, v/v) was performed to give 1.30 g (yield 75.3%) of product. $^1$H NMR (400 MHz, $CDCl_3$): δ 6.34 (s, 2H), 4.24 (d, 2H, *J*=9.6 Hz), 4.07-4.12 (m, 1H), 3.84-3.87 (m, 2H).

*2.2.4 N-(tert-butoxycarbonyl)-L-alanine (N-Boc-L-Ala)*

A solution of $(Boc)_2O$ (25.91 g, 118.72 mmol) in dioxane (90 mL) was added to an ice-cold solution of L-alanine (8.91 g, 100.01 mmol) in 1 M NaOH (200 mL) with stirring. After 30 min at -3 °C, the mixture was warmed to room temperature over 14 h with stirring. The mixture was concentrated to half its original volume by rotary evaporation, cooled in ice, and acidified to pH 2-3 by slow addition of 1 M cold $NaHSO_4$. Then extracted with acetic ether 200 mL×3, the combined extracts were dried with $MgSO_4$, filtered, and concentrated to give 17.45 g of a colorless solid.

*2.2.5 EDOT-Boc-Ala*

To a three-necked flask, EDOT-MeOH (2.58 g, 14.98 mmol), DCC (3.28 g, 15.90 mmol), and DMAP (0.13 g, 1.06 mmol) were dissolved in DCM (75 mL) with stirring while being cooled in an ice bath. N-Boc-L-Ala (3.0 g, 15.86 mmol) which was dissolved in DCM (20 mL) was added slowly to the cooled solution. After stirring for 1 h, the ice bath was removed and the reaction continued at room temperature. After another 16 h, the colorless precipitate 1,3-dicyclohexylurea was filtered off and discarded. The clear, colorless solution was washed with 1 M HCl 90 mL×3, saturated solution of sodium bicarbonate ($NaHCO_3$) 90 mL×3, and then with saturated brine 90 mL×3. The organic layer was dried with $Na_2SO_4$ and filtered. The solvent was removed under reduced pressure and column chromatography (petroleum ether/acetic ether, 4/1, v/v) was performed to give 4.85 g (yield 94.2%) of product. $[\alpha]^{20.0} = -30.77°$. $^1$H NMR (400 MHz, $CDCl_3$): δ 7.34 (s, 1H), 6.58 (s, 2H), 4.31-4.36 (m, 4H), 3.97-4.01 (m, 2H), 1.34 (s, 9H), 1.19 (d, 3H, *J*=18.8 Hz).

*2.3. Electrochemical Measurements*

Electrochemical synthesis and examinations were performed in a one-compartment cell with the use of Model 263 potentiostat-galvanostat (EG&G Princeton Applied Research) under computer control. All the three electrodes were platinum (Pt) wires with a diameter of 0.5 mm, respectively. The three electrodes were placed 5 mm apart during the measurements. To obtain a sufficient amount of polymer for characterization, the Pt sheets with a surface area of 10 and 12 $cm^2$ each (10 mm apart) were employed as working and counter electrodes, respectively. The Pt wire electrode directly immersed in the solution served as the reference electrode and it revealed sufficient stability during the experiments. Electrodes mentioned above were carefully polished with abrasive paper (1500 mesh), and cleaned by water and acetone successively before each examination. All experiments were carried out under a slight argon overpressure. Finally, the polymer film was dried at 60 °C under vacuum for 24 h. The PEDOT-Boc-Ala film was prepared in DCM containing 0.02 M EDOT-Boc-Ala and 0.10 M

$Bu_4NBF_4$ and characterized electrochemically in monomer-free DCM containing 0.10 M $Bu_4NBF_4$.

### *2.4 Fabrication of biosensor*

To fabricate a biosensor, a Pt disc electrode was used as the working electrode. The PEDOT-Boc-Ala film was prepared potentiostatically at 1.1 V in DCM. The obtained PEDOT-Boc-Ala modified Pt disc electrode was washed repeatedly with double-distilled deionized water to remove the electrolyte and monomer. Then 5 μL of 250 U AO was dip-coated on the surface of the PEDOT-Boc-Ala modified Pt disc electrode using a finnpipette. PEDOT-Boc-Ala/AO modified Pt disc electrode was dried in air, and then 5 μL of 0.5% nafion was dip-casted onto the surface of AO layer and dried in air. Finally, the prepared PEDOT-Boc-Ala/AO/nafion modified Pt disc electrode was stored in 50 mM PBS at 4 °C when not in use. The working parameters of the fabricated biosensor were selected according to our previous studies [43-45].

### *2.5. Characterizations*

NMR spectra were recorded on a Bruker AV 400 NMR spectrometer with $d_6$-DMSO as the solvent and tetramethylsilane as an internal standard (TMS, singlet, chemical shift: 0.0 ppm). Infrared spectra (FT-IR) were recorded using Bruker Vertex 70 Fourier spectrometer with samples in KBr pellets. Ultraviolet-visible (UV-vis) spectra were measured with a Perkin-Elmer Lambda 900 ultraviolet-visible-near-infrared spectrophotometer. Optical rotation determination was performed on Anton Paar MCP 200 polarimeter. With an F-4500 fluorescence spectrophotometer (Hitachi), fluorescence spectra of the monomer and polymer were determined. Thermogravimetric (TG) and differential thermogravimetric (DTG) analysis was performed with a Pyris Diamond TG/DTA thermal analyzer (Perkin-Elmer). Scanning electron microscopy (SEM) measurements were taken using Sigma cold field emission scanning electron microscope. The addition of solutions to the cell was performed with the Finnpipette (Labsystems, Helsinki, Finland). pH values were measured with a Delta 320 pH meter (Mettler-Toledo Instrument, Shanghai, China). The temperature was controlled with a type HHS thermostat (Shanghai, China).

## 3. RESULTS AND DISCUSSION

### *3.1 Synthesis of EDOT-MeOH*

The synthesis of EDOT-MeOH is the key to synthesize the precursor PEDOT-Boc-Ala. Until now, most of literatures have always used the method reported by Chevrot and co-workers [46-47] to make EDOT-MeOH, but the procedure involved six steps starting from thiodiglycolic acid, which needs complex operation and also leads to a low total yield. Meanwhile, an isomeric hydroxyl-substituted 3,4-propylenedioxythiophene was formed as a byproduct, which could be separated only after tedious chromatographic purification. Therefore, we prepared EDOT-MeCl from 3,4-

dibromothiophene first and then adopting the approach described by Yeisley et al [42] synthesized EDOT-MeOH. This reaction route has advantages of commercially available reactants, few steps, ease of operation, low cost, and so on.

### *3.2. Electrochemical polymerization*

The electrochemical performances of EDOT-Boc-Ala were studied in DCM–$Bu_4NBF_4$. The consecutive cyclic voltammograms (CVs) of EDOT-Boc-Ala is shown in Figure 1.

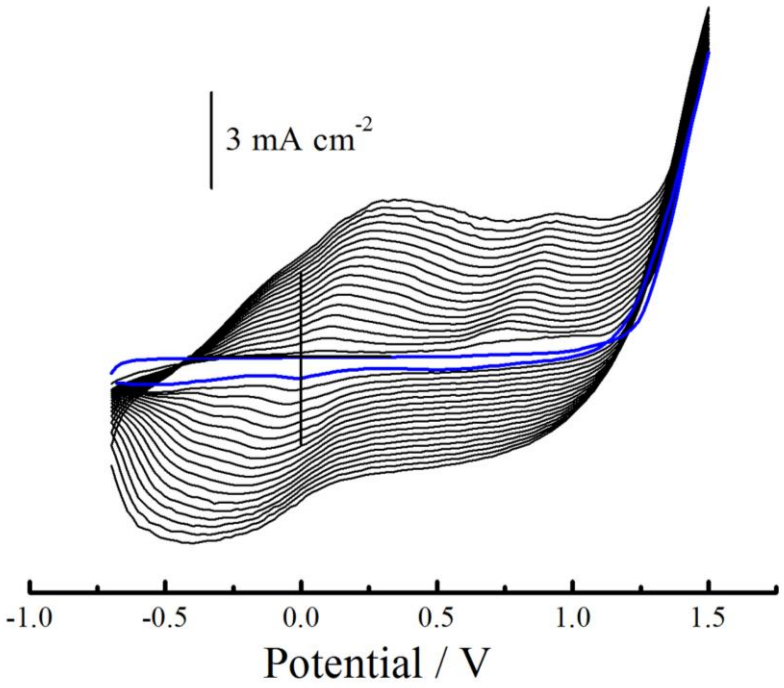


**Figure 1.** CVs of EDOT-Boc-Ala monomer. Potential scan rate: 100 mV $s^{-1}$.

In the first cycle of CVs, the current densities on the reverse scan were higher than on the forward scan (in the region of 1.0-1.5 V). The formation of this loop could be explained as the characteristics of nucleation process. The redox peaks at 0.8 V and -0.4 V were attributed to the p-doping/dedoping process of PEDOT-Boc-Ala film formed in previous scans. Upon sequential cycles, redox currents increased, implying that the formation of an electroactive and conductive layer on the Pt electrode surface (light-blue to blue-black as the deposit thickened) was gradually increasing. The broad redox waves of the as-formed PEDOT-Boc-Ala film could be ascribed to the wide distribution of the polymer chain length or the version of conductive species on the polymer main chain from the neutral state to polarons, from polarons to bipolarons, and finally from bipolarons to the metallic state [48]. The potential shift of the current wave maximum provided information about the increase of the electrical resistance of the polymer film and the overpotential needed to overcome this resistance.

### *3.3. Electrochemistry of PEDOT-Boc-Ala film*

For insight into the electroactivity of the obtained polymer film, the electrochemical behavior of PEDOT-Boc-Ala-modified electrode was investigated carefully by cyclic voltammetry in monomer-free DCM–$Bu_4NBF_4$ (Figure 2). The modified electrode represented steady-state and broad redox peaks (both anodic and cathodic) in monomer-free electrolytes. This might be ascribed to the presence of slow diffusion of the counterions inside the film, changes of the film capacitance, and a wide distribution of the polymer chain length resulting from coupling defects distributed statically [49]. The peak current densities were linearly proportional to the potential scanning rates (Figure 2 inset), indicating that the redox process was non-diffusional and the electroactive polymer was well adhered to the working electrode surface. Meanwhile, the conducting (oxidized) and insulating (neutral) state without significant decomposition of the materials, indicating high stability of the polymer.

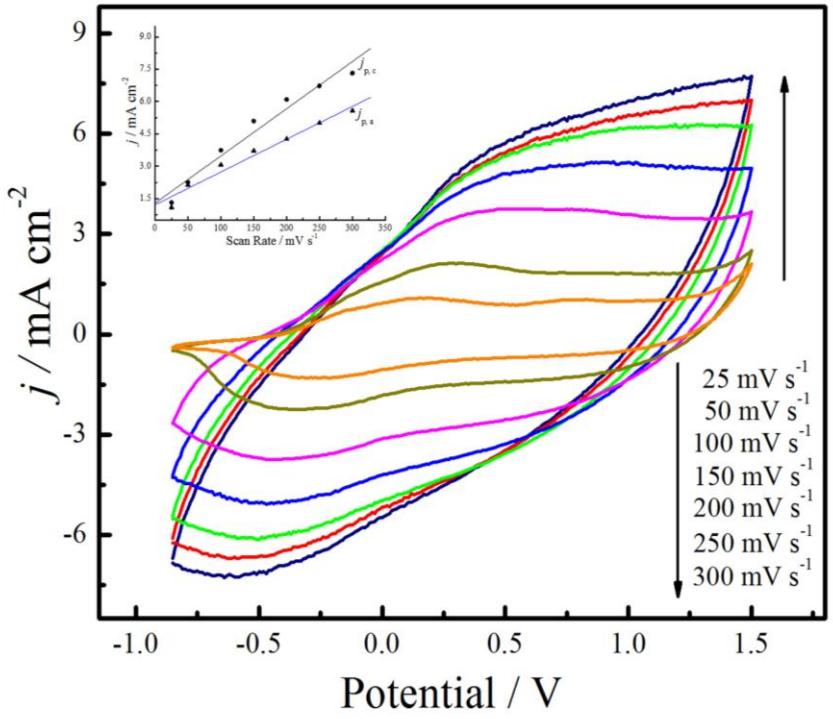


**Figure 2.** CVs of PEDOT-Boc-Ala film on platinum wire electrode in monomer-free DCM–$Bu_4NBF_4$ at different potential scan rates. The film was obtained by CV. Inset: plots of redox peak current densities *vs* potential scan rates. $j_p$ is the peak current densities, $j_{p.a}$ and $j_{p.c}$ denote the anodic and the cathodic peak current densities, respectively.

### *3.4. Infrared spectra*

Infrared spectra can provide much structural information for conducting polymers, and may be used to interpret the polymerization mechanism, especially for insoluble and infusible conducting polymers. The comparison of the evolution of vibrational modes in polymer and in some simpler related molecules acting as references usually facilitates the interpretation of the experimental absorption spectra. Therefore, typical FT-IR spectra of the monomer (a) and both doped (b) and

dedoped (c) polymer were illustrated in Figure 3. The peaks at 3123 $cm^{-1}$, 1750 $cm^{-1}$, 1516 $cm^{-1}$, and 1172 $cm^{-1}$ were closely related to the bond of N-H of the monomer (Figure 3a), which were shifted to 3010 $cm^{-1}$, 1745 $cm^{-1}$, 1516 $cm^{-1}$, and 1200 $cm^{-1}$ in the doped polymer (Figure 3b) and 1740 $cm^{-1}$, 1516 $cm^{-1}$, 1200 $cm^{-1}$ in the dedoped polymer (Figure 3c). The strong and broad peak at 1715 $cm^{-1}$ was characteristic of C=O bond, which was shifted to 1746 $cm^{-1}$ (Figure 3b) and 1745 $cm^{-1}$ (Figure 3c) in the doped and dedoped polymer, respectively.

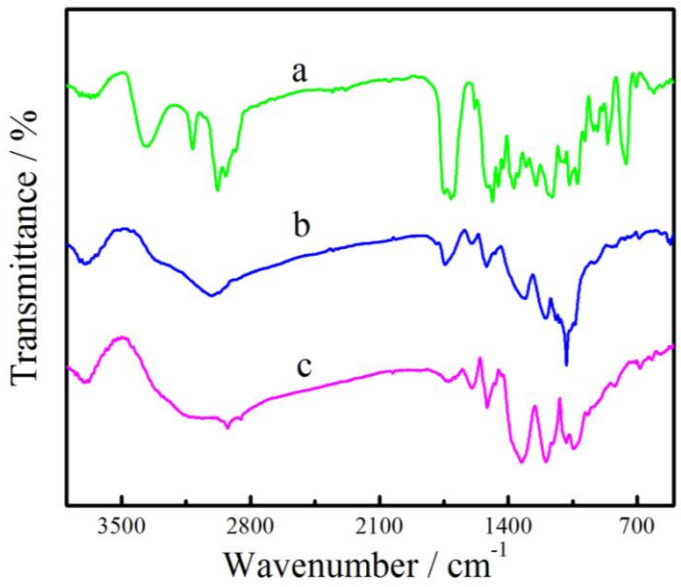


**Figure 3.** FT-IR spectra of EDOT-Boc-Ala (a), doped PEDOT-Boc-Ala (b) and dedoped PEDOT-Boc-Ala (c).

All results confirmed that the structure of EDOT-Boc-Ala was not destroyed during the electrochemical polymerization process. However, the peak of EDOT-Boc-Ala at 762 $cm^{-1}$ (Figure 3a) obviously was weakened compared with that of the doped and dedoped PEDOT-Boc-Ala (Figure 3b and 3c), which might be attributed to the electrochemical polymerization of EDOT-Boc-Ala occurring at the "2" and "5" position of the thiophene ring. Moreover, the augmented width and shifts of these bands from the monomer to polymer manifested the occurrence of the electrochemical polymerization of EDOT-Boc-Ala. The broadening of the IR bands in the experimental spectra was due to the resulting product composed of oligomers with wide chain dispersity. The vibrational peaks of the oligomers with different polymerization degrees had different IR shifts. These peaks overlapped one another and produced broad bands with hyperstructures. Furthermore, there were chemical defects on the polymer chains, which resulted from the inevitable overoxidation of the polymer. This also contributed to the band broadening of IR spectra [50].

### *3.5. UV-vis spectra*

The as-prepared PEDOT-Boc-Ala film in the doped state was metallic dark blue in color. When

the film was dedoped by 25% ammonia for 3 days, its color changed to brownish yellow. In addition, the resulting PEDOT-Boc-Ala film was found to be thoroughly soluble in DMSO or THF, and also exhibited good solubility in other solvents such as acetonitrile, and acetone. The gel chromatography determination showed that the number average molecular weight was 6100, the weight average molecular weight was 8400, and the dispersion index was 1.37. This nice solubility of PEDOT-Boc-Ala may facilitate its applications in various fields and also benefit its further postfunctionalization.

UV-vis spectra of the monomer and the resulting polymer dissolved in DMSO were examined in Figure 4.

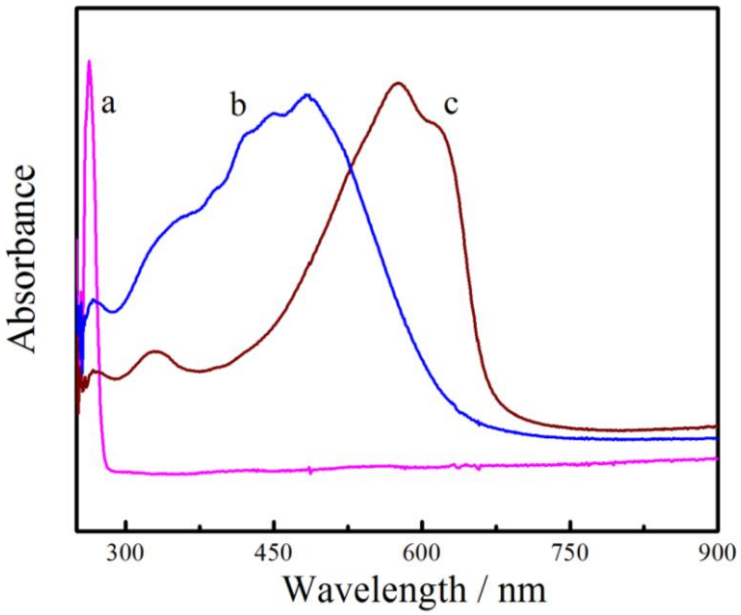


**Figure 4.** UV-vis spectra of the monomer and its polymer in DMSO. a: EDOT-Boc-Ala , b: doped PEDOT-Boc-Ala , c: dedopod PEDOT-Boc-Ala.

The monomer showed a characteristic absorption peak at 263 nm (Figure 4a), while the spectra of the doped and dedoped PEDOT-Boc-Ala film showed a much broader absorption with their maximum at 483 nm (Figure 4b) and 575 nm (Figure 4c), respectively. The overall absorption of PEDOT-Boc-Ala tailed off to more than 720 nm (Figure 4b and 4c). Generally, the longer wavelength is the absorption, the higher conjugation length is the polymer. These spectral results confirmed the occurrence of the electrochemical polymerization among the monomer and the formation of a conjugated polymer with broad molar mass distribution. Furthermore, the optical band gap of PEDOT-Boc-Ala calculated from the onset of the absorption spectrum (about 720 nm) was roughly 1.72 eV (Eg = 1241/λonset).

### *3.6. Chiroptical property*

The optical rotation of the monomer and PEDOT-Boc-Ala film dissolved in DMSO was

studied, as listed in Table 1. In comparison with the specific rotation of monomer (-30.77°), the resulting polymer exhibited much larger specific rotation (-191.08°), indicating that the trans conformation of the monomer was not destroyed during the electrochemical polymerization. The enhanced rotation may be ascribed to the following reasons: (1) after polymerization, the accumulation of L-alanine groups in the side chain increases the specific rotation of the polymer; (2) the presence of enantiomerically pure L-alanine substituents may induce optical activity to the polymer, as in the cases of a wide range of chiral polypyrroles and polythiophenes [4]. Based on above results, a trans main chain conformation with enhanced chirality can be assigned to the polymer. In addition, in comparison with PEDOT, the resulting chiral PEDOT-Boc-Ala is a potential candidate as a chiral substrate or as a chiral electrode material and could, for example, find application in electrochemical chiral sensing or electrochemical asymmetric synthesis.

**Table 1.** Optical rotations of EDOT-Boc-Ala and dedoped PEDOT-Boc-Ala. Solvent: DMSO.

| Sample | Polymerization condition | C / g/dL | T / °C | $[\alpha]_D$ (C = 1, DMSO) |
|---|---|---|---|---|
| EDOT-Boc-Ala | - | 0.8320 | 20.0 | -30.77° |
| PEDOT-Boc-Ala | 1.5 V (Pt) | 0.0157 | 20.0 | -191.08° |

*3.7. Fluorescent property*

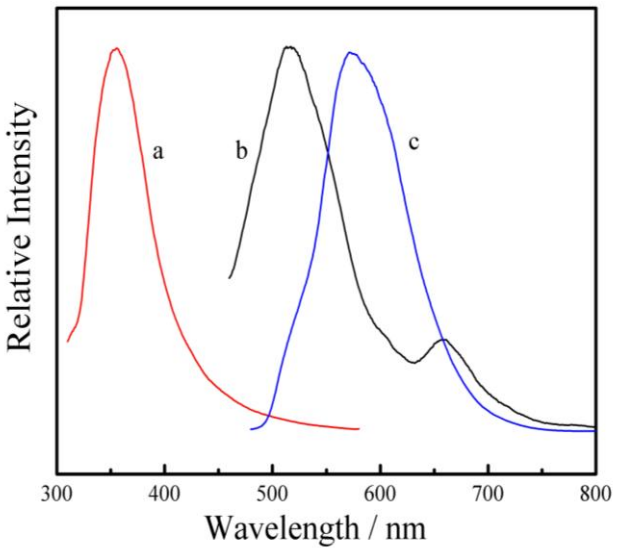


**Figure 5.** Fluorescence spectra of the monomer and its polymer in DMSO. a: EDOT-Boc-Ala, b: doped PEDOT-Boc-Ala, c: dedoped PEDOT-Boc-Ala.

Figure 5 shows the fluorescence emission spectra of the monomer and polymer in the doped and dedoped states dissolved in DMSO. It is observed that the emission peak of the monomer emerged at 356 nm, whereas the dominant maximum emission at 516 and 571 nm characterized the spectra of

the doped (Figure 5b) and dedoped (Figure 5c) PEDOT-Boc-Ala, respectively. The very large red shifts between the monomer and the polymer (about 160 nm) could be clearly seen from Figure 5, which was mainly attributable to the elongation of the polymer delocalized π-electron chain sequence. Another peak at 660 nm characterized the spectra of the doped PEDOT-Boc-Ala (Figure 5b), which was mainly attributable to the doped ion compared to the dedoped polymer (Figure 5c). Moreover, the wider emission spectrum of the oligomer could be attributable to the wide molar mass distribution of PEDOT-Boc-Ala. Based on above results, the polymer was a typically good green-light-emitting polymer.

*3.8. Thermal analysis*

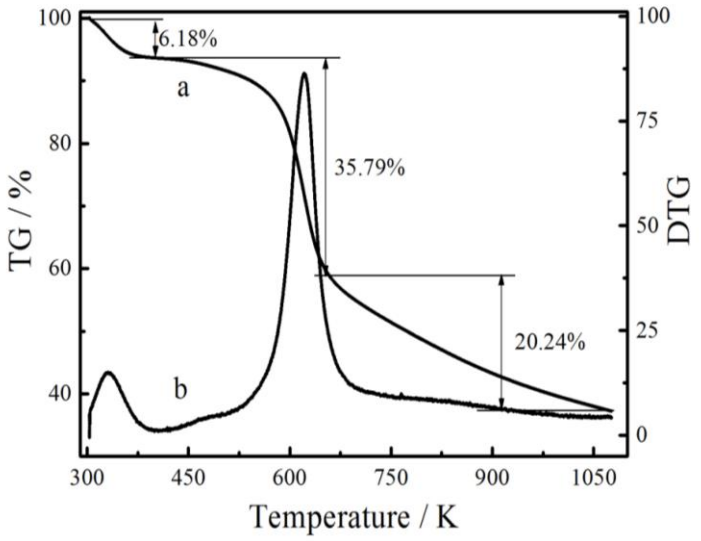


**Figure 6.** TG/DTG curves of dedoped PEDOT-Boc-Ala film.

To investigate the thermal stability of the prepared PEDOT-Boc-Ala film, TG and DTG experiments were performed under nitrogen protection at a heating rate of 10 K $min^{-1}$, as shown in Figure 6. At low temperatures ($T \leq 400$ K), the weight loss of PEDOT-Boc-Ala film was about 6.38% due to evaporation of trace water or other moisture trapped in the polymer. As the temperature continued increasing, a more pronounced weight loss step (35.79%) was observed for 400 K < $T \leq 659$ K. Meanwhile, the DTG curve showed that the corresponding maximal decomposition occurred at 623 K. Such a weight loss was closely related to the degradation of some oligomers or PEDOT-Boc-Ala side chain structure. Secondarily, the degradation above 659 K amounting to 20.24% was probably caused by the oxidizing decomposition of skeletal PEDOT-Boc-Ala backbone chain structure. Therefore, the as-prepared PEDOT-Boc-Ala film had good thermal stability, which is of special significance for some potential application.

*3.9. Surface morphology*

The surface morphology of PEDOT-Boc-Ala film prepared in DCM–$Bu_4NBF_4$ on ITO transparent electrode at a constant potential of 1.5 V was presented in Figure 7. The prepared film presented a dense, compact, and homogeneous structure. There was obvious difference in surface morphology of the doped/dedoped PEDOT-Boc-Ala film. The surface morphology of the doped polymer film is very smooth in Figure 7a, while the dedoped polymer film (Figure 7b) became uneven and cracking. This phenomenon was due to the migration of counteranions out of the polymer film during the dedoping process, which broke the smooth surface of the doped PEDOT-Boc-Ala film. In addition, the surface structure of the doped PEDOT-Boc-Ala film was similar to that of PEDOT [51,52], which will be beneficial to the design and fabrication of the sensing and biosensing devices.

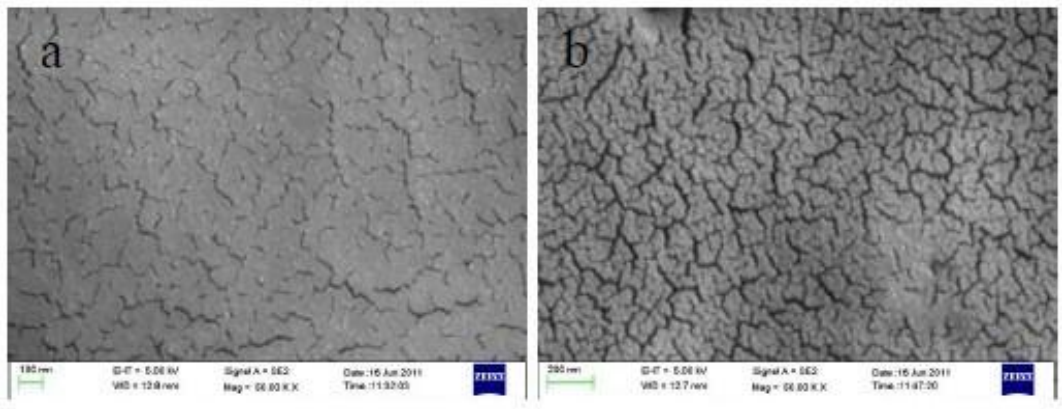


**Figure 7.** SEM images of PEDOT-Boc-Ala film electrodeposited on ITO electrode for 40 s. a: doped PEDOT-Boc-Ala, b: dedoped PEDOT-Boc-Ala.

*3.10. Sensing application of PEDOT-Boc-Ala film*

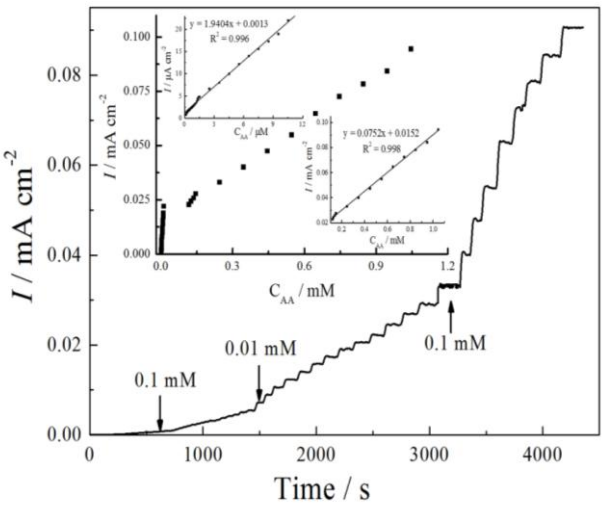


**Figure 8.** The constant potential amperometric response curves of AA at 0.4 V in oxygen saturated PBS under stable stirring condition at room temperature.

PEDOT-Boc-Ala film as the immobilization matrix of biologically-active species was employed for the fabrication of the amperometric biosensor, and AO was selected as a model. The fabricated biosensor based on the PEDOT-Boc-Ala matrix was applied for the detection of AA. The concentration of $O_2$ was kept constantly by air-saturating buffer solutions because $O_2$ was a co-substrate of AO catalytic reaction. The steady-state current response increased with the increasing concentration of AA (Figure 8), revealing that AA could be successfully detected by the fabricated biosensor. The linear range of the steady-state current response (I) − the concentration of AA ([AA]) was defined at lower concentration.

Figure 8 shows the constant potential amperometric response curves of AA at 0.4 V in $O_2$−saturated PBS under stable stirring condition at room temperature. The results indicated that this biosensor exhibited an excellent current response for AA with short response time (within 10 s). Good linear relationship was observed between [AA] and I in the concentration range of 0.1 μM to 10.5 μM ($y = 1.9404\ x + 0.0013$, $r = 0.996$) and 10.5 μM to 1.05 mM ($y = 0.0752\ x - 0.0152$, $r = 0.9998$), respectively. The sensitivity (from the slope of the linear part in Figure 8 inset) was 1.9404 and 0.0752 mA $mM^{-1}$ $cm^{-2}$, respectively. And the lowest detection limitation of the fabricated biosensor is 0.063 μM. In addition, the higher concentration of AA was not studied owing to the consumption of the dissolved $O_2$ amounts in surrounding enzymes resulting in a gradual deviation from linearity according to our previous reports [43-45]. The good results described above indicated that this method is suitable for detecting the unknown [VC] and could determine the content of VC in plants within the narrow limitations of $2\times10^{-3}$ to $2.5\times10^{-2}$ M [53].

## 4. CONCLUSIONS

To summarize, the precursor chiral EDOT-Boc-Ala was synthesized and electrochemically polymerized for the first time. The corresponding polymer PEDOT-Boc-Ala showed good redox activity and stability in monomer-free electrolytes. Structural characterization demonstrated that a novel chiral PEDOT derivative with enhanced main chain chirality ($[\alpha]^{20.0} = -191.08^{o}$) was obtained. Fluorescent spectral studies indicated that PEDOT-Boc-Ala was a good green-light emitter with maximum emission centered at 516 nm and 571 nm. Moreover, the thermal behavior and surface morphology of PEDOT-Boc-Ala were characterized. Inspired by the preceding studies, PEDOT-Boc-Ala was employed for the fabrication of the AO-based biosensor and the fabricated biosensor displayed good biosensing performances for the detection of vitamin C. These attractive properties of PEDOT-Boc-Ala film mentioned above will benefit its potential application in organic electronic devices, enantioselective catalysis, asymmetric synthesis, sensing and biosensing devices, etc. Further functionalization of the precursor and the resulting polymer to improve its properties and performances is also in progress.

ACKNOWLEDGMENTS

The authors would like to acknowledge the financial support of this work by the National Natural Science Foundation of China (51263010, 51272096, 51073074), Natural Science Foundation of

Jiangxi Province (20114BAB203015, 20122BAB216011, 2010GZH0041), and Jiangxi Provincial Department of Education (GJJ10678, GJJ12595, GJJ11590).

## References

1. T. Nakano and Y. Okamoto, *Chem. Rev.* 101 (2001) 4013.
2. J. J. L. M. Cornelissen, A. E. Rowan, R. J. M. Nolte and N. A. J. M. Sommerdijk, *Chem. Rev.* 101 (2001) 4039.
3. H. Shirakawa, E. J. Louis, A. G. MacDiarmid, C. K. Chiang and A. J. Heeger, *J. Chem. Soc., Chem. Commun.* (1977) 578.
4. L. A. P. Kane-Maguire and G. G. Wallace, *Chem. Soc. Rev.* 39 (2010) 2545.
5. C. D. McTiernan, K. Omri and M. Chahma, *J. Org. Chem.* 75 (2010) 6096.
6. Y. Okamoto and T. Nakano, *Chem. Rev.* 94 (1994) 349.
7. R. J. M. Nolte, *Chem. Soc. Rev.* 23 (1994) 11.
8. G. Wulff, *Angew. Chem., Int. Ed. Engl.* 34 (1995) 1812.
9. L. Pu, *Chem. Rev.* 104 (2004) 1687.
10. B. Y. Lu, J. K. Xu, Y. Z. Li, C. C. Liu, R. R. Yue and X. X. Sun, *Electrochim. Acta* 55 (2010) 2391.
11. E. Yashiama, K. Maeda and Y. Okamoto, *Nature* 399 (1999) 449.
12. K. Maeda, S. Okada, E. Yashima and Y. Okamoto, *J. Polym, Sci., Part A: Polym. Chem.* 39 (2001) 3180.
13. M. Ishikawa, K. Maeda and E. Yashima, *J. Am. Chem. Soc.* 124 (2002) 7448.
14. L. Chen, Y. Chen, K. Yao, W. Zhou, F. Li, L. Chen, R. Hu and B. Z. Tang, *Macromolecules* 42 (2009) 5053.
15. M. Goh, S. Matsushita and K. Akagi, *Chem. Soc. Rev*. 39 (2010) 2466.
16. J. Z. Liu, J. W. Y. Lam and B. Z. Tang, *Chem. Rev.* 109 (2009) 5799.
17. Y. S. Jeong, H. Goto, S. Iimura, T. Asano and K. Akagi, *Curr. Appl. Phys*. 6 (2006) 960.
18. K. Akagi, G. Piao, S. Kaneko, K. Sakamaki, H. Shirakawa and M. Kyotani, *Science* 282 (1998) 1683.
19. M. Goh, T. Matsushita, M. Kyotani and K. Akagi, *Macromolecules* 40 (2007) 4762.
20. T. Mori, T. Sato, M. Kyotani and K. Akagi, *Macromolecules* 42 (2009) 1817.
21. J. F. Hulvat and S. I. Stupp, *Angew. Chem., Int. Ed*. 42 (2003) 778.
22. J. F. Hulvat and S. I. Stupp, *Adv. Mater*. 16 (2004) 589.
23. D. Iarossi, A. Mucci, F. Parenti, L. Schenetti, R. Seeber, C. Zanardi, A. Forni and M. Tonelli, *Chem. Eur. J*. 7 (2001) 676.
24. M. Lemaire, D. Delabouglise, R. Garreau, A. Guy and J. Roncali, *J. Chem. Soc., Chem. Commun*. (1988) 658.
25. D. Kotkar, V. Joshi and P. K. Ghosh, *J. Chem. Soc., Chem. Commun*. (1988) 917.
26. M. M. Bouman, E. E. Havinga, R. A. J. Janssen and E. W. Meijer, *Mol. Cryst. Liq. Cryst*. 256 (1994) 439.
27. M. M. Bouman and E. W. Meijer, *Adv. Mater*. 7 (1995) 385.
28. G. Bidan, S. Guillerez and V. Sorokin, *Adv. Mater*. 8 (1996) 157.
29. Z. B. Zhang, M. Fujiki, M. Motonaga, H. Nakashima, K. Torimitsu and H. Z. Tang, *Macromolecules* 35 (2002) 941.
30. B. M. W. Langeveld-Voss, R. A. J. Janssen, M. P. T. Christiaans, S. C. J. Meskers, H. P. J. M. Dekkers and E. W. Meijer, *J. Am. Chem. Soc*. 118 (1996) 4908.
31. B. M. W. Langeveld-Voss, R. A. J. Janssen and E. W. Meijer, *J. Mol. Struct*. 521 (2000) 285.
32. A. F. M. Kilbinger, A. P. H. J. Schenning, F. Goldoni, W. J. Feast and E. W. Meijer, *J. Am. Chem. Soc.* 122 (2000) 1820.

33. H. Goto and E. Yashima, *J. Am. Chem. Soc*. 124 (2002) 7943.
34. D. Caras-Quintero and P. Bauerle, *Chem. Commun*. (2004) 926.
35. D. Caras-Quintero and P. Bauerle *Chem. Commun*. (2002) 2690.
36. C. R. G. Grenier, S. J. George, T. J. Joncheray, E. W. Meijer and J. R. Reynolds, *J. Am. Chem. Soc.* 129 (2007) 10694.
37. H. Brisset, A. -E. Navarro, C. Moustrou, I. F. Perepichka and J. Roncali, *Electrochem. Commun*. 6 (2004) 249.
38. M. Döbbelin, C. Pozo-Gonzalo, R. Marcilla, R. Blanco, J. L. Segura, J. A. Pomposo and D. Mecerreyes, *J. Polym. Sci., Part A: Polym. Chem*. 47 (2009) 3010.
39. R. R. Yue, B. Y. Lu, J. K. Xu, S. Chen and C. C. Liu, *Polym. J.* 43 (2011) 531.
40. S. Yeisley, C. J. Dubois, C. Hsu, S. W. Shuey, Y. L. Shen and H. Skulason, US Patent (2011) 7999121.
41. J. L. Segura, R. Gómez, R. Blanco, E. Reinold, and P. Bäuerle, *Chem. Mater*. 18 (2006) 2834.
42. K. Velauthamurty, S. J. Higgins, R. M. G. Rajapakse, J. Bacsa, H. van Zalinge, R. J. Nicholsa and W. Haiss, *J. Mater. Chem*. 19 (2009) 1850.
43. M. Liu, Y. P. Wen, D. Li, H. H. He, J. K. Xu, C. C. Liu, R. R. Yue, B. Y. Lu and G. D. Liu, *J. Appl. Polym. Sci*. 122 (2011) 1142.
44. M. Liu, Y. P. Wen, J. K. Xu, H. H. He, D. Li, R. R. Yue, B. Y. Lu and G. D. Liu, *Anal. Sci.* 27 (2011) 477.
45. M. Liu, Y. P. Wen, D. Li, R. R. Yue, J. K. Xu and H. H. He, *Sensor. Actuat. B-Chem*. 159 (2011) 277.
46. A. Lima, P. Schottland, S. Sadki and C. Chevrot, *Synth. Met*. 93 (1998) 33.
47. [47] O. Stéphan, P. Schottland, P. L. Gall, C. Chevrot, C. Mariet and M. Carrier, *J. Electroanal. Chem.* 443 (1998) 217.
48. M. Zhou and J. Heinze, *Electrochim. Acta*. 44 (1999) 1733.
49. G. Inzelt, M. Pineri, J.W. Schultze, M.A. Vorotyntsev, *Electrochim. Acta* 45 (2000) 2403.
50. J. X. Zhang, C. Liu, G. Q. Shi, Y. F. Zhao, *J. Polym. Sci. Part B: Polym. Phys.* 43 (2005) 241–251.
51. S. S. Zhang, J. Hou, R. Zhang, J. K. Xu, G. M. Nie and S. Z. Pu, *Eur. Polym. J.* 42 (2006) 149.
52. Y. P. Wen, J. K. Xu, H. H. He, B. Y. Lu, Y. Z. Li and B. Dong, *J. Electroanal. Chem*. 634 (2009) 49.
53. N. Smirnoff, *Curr. Opin. Plant. Biol*. 3 (2000) 229.